THE EUROPEAN
PHYSICAL JOURNAL A

Infrared gluon and ghost propagators from lattice QCD

Results from large asymmetric lattices

O. Oliveira[a] and P.J. Silva

Centro de Física Computacional, Universidade de Coimbra, 3004 516 Coimbra, Portugal

Abstract. We report on the infrared limit of the quenched lattice Landau gauge gluon and ghost propagators as well as the strong-coupling constant computed from large asymmetric lattices. The infrared lattice propagators are compared with the pure power law solutions from Dyson-Schwinger equations (DSE). For the gluon propagator, the lattice data is compatible with the DSE solution. The preferred measured gluon exponent being ~ 0.52, favouring a vanishing propagator at zero momentum. The lattice ghost propagator shows finite-volume effects and, for the volumes considered, the propagator does not follow a pure power law. Furthermore, the strong-coupling constant is computed and its infrared behaviour investigated.

PACS. 12.38.-t Quantum chromodynamics – 11.15.Ha Lattice gauge theory – 12.38.Gc Lattice QCD calculations – 14.70.Dj Gluons

1 Introduction

In the pure gauge $SU(3)$ Yang-Mills theory, a number of authors has been using first principles approaches, *i.e.* Dyson-Schwinger equations (DSE) and lattice QCD methods, to investigate the infrared gluon and ghost propagators in Landau gauge, respectively,

$$D_{\mu\nu}^{ab}(k) = \delta^{ab}\left(\delta_{\mu\nu} - \frac{k_\mu k_\nu}{k^2}\right)D(k^2),\qquad(1)$$

$$G_{\mu\nu}^{ab}(k) = -\delta^{ab}G(k^2),\qquad(2)$$

and the strong-coupling constant [1] defined as

$$\alpha_S(k^2) = \alpha_S(\mu^2)\, Z_{ghost}^2(k^2)\, Z_{gluon}(k^2);\qquad(3)$$

$Z_{ghost}(k^2) = k^2 G(k^2)$ and $Z_{gluon}(k^2) = k^2 D(k^2)$ are the ghost and gluon dressing functions. In part, these studies have been trigered by the solution of the DSE [2] which assuming infrared ghost dominance and infrared finiteness of the loop-integrals predicts pure power laws for the dressing functions

$$Z_{gluon}(k^2) = A\left(k^2\right)^{\kappa'},\quad Z_{ghost}(k^2) = B\left(k^2\right)^{-\kappa}.\quad(4)$$

Moreover, the DSE solution relates the exponents of the two propagators, $\kappa' = 2\kappa$, and predicts a finite strong-coupling constant at zero momentum. The infrared solution predicts a vanishing gluon propagator and an infinite ghost propagator at zero momentum ($\kappa > 0.5$). The
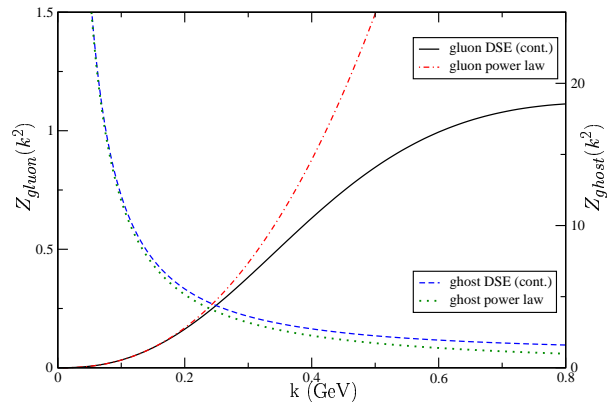
Fig. 1. DSE gluon and ghost dressing functions *versus* the pure power law solutions. The data is taken from [3].

infrared behaviour of the propagators can be related to gluon confinement criteria [4]. Looking at this particular DSE solution for the gluon propagator, the comparison with the pure power law, see fig. 1, shows that the pure power law is valid only for momenta $k < 200\,\text{MeV}$. Notice that for the ghost, the deviations from a pure power law start earlier.

One should have in mind that the solution discussed above is a particular solution of the DSE. Indeed, there are, in the literature, different types of solutions for the DSE [5]. Moreover, the authors of [6] have investigated a generalization of the conditions assumed in [2] and found alternative behaviours for the infrared gluon and ghost propagators. Given the different scenarios, it would be im-

[a] e-mail: orland@teor.fis.uc.pt

portant if lattice QCD can provide additional input, help-
ing to check if any of the proposed solutions reproduces
the lattice data. For a recent discussion on the infrared
behaviour of the gluon and ghost propagators see [7].

For the lattice it is a challenge to investigate such low
momenta. A possible way out is to consider large asym-
metric lattices, which allows to access the momenta re-
quired in such an investigation [8–11]. Of course, there are
lattice effects that have to be carefully estimated. Here we
report on the gluon, ghost and strong-coupling constant
computed from large asymmetric lattices.

2 Gluon propagator

In [11] we have investigated the infrared lattice Landau
gauge gluon propagator. For notation and definitions see
the above cited article. The simulation uses the Wilson
action with $\beta = 6.0$ and combines a number of asymmet-
ric lattices $L^3 \times 256$, $L = 8, 10, 12, 14, 16, 18$ to allow for
$L \to +\infty$ extrapolation. In what concerns the time direc-
tion, the $16^3 \times 256$ and $16^3 \times 128$ gluon propagators were
compared and no deviations were observed. This suggests
that we have a sufficient number of points in the time
direction.

For the lattices with the largest time direction, the
minimum momentum being accessed is 47 MeV, while for
the $16^3 \times 128$ the minimum momentum is 98 MeV. For the
largest lattices with $T = 256$ a pure power law in the in-
frared is observed. In contrast, for the lattice of $16^3 \times 128$,
power law fits are very poor with $\chi^2/\text{d.o.f} > 10$. This re-
sult is not surprising, given the smallest range of momenta
available for this lattice (97–294 MeV) and the validity of
the pure power law. Nevertheless, the $16^3 \times 128$ will al-
low us to estimate Gribov copies effects, with reasonable
computational effort.

Let us summarize the results reported in [11] using the
simulations with the largest time extension. Asymmetric
lattices display finite size effects (see figs. 4 and 5 of [11]).
However, the extrapolation towards $L \to +\infty$ is smooth.
The extrapolated gluon propagator was well reproduced
by a pure power law, with measured $\kappa = 0.49$–0.52.
Clearly, the lattice data favors $\kappa \sim 0.52$, in agreement
with other theoretical estimates. Unfortunately, one can-
not yet provide a definitive answer concerning the value of
the gluon propagator at zero momentum. We are currently
engaged in trying to give such an answer.

For the $16^3 \times 128$ lattice, Gribov copies effects were
estimated by comparing the gluon propagator computed
from 164 configurations gauge fixed as in [11] (SD in the
figures) and the same gauge configurations gauge fixed
using the method described in [12] (CEASD in the fig-
ures), which aims to estimate the absolute maximum of
the gauge fixing function. The gluon propagator given by
the two methods is, within the statistical precision of the
simulation, the same (see fig. 2), with the various fits to
the lattice data (infrared, ultraviolet, all momenta) re-
producing similar results. Therefore, no visible effects of
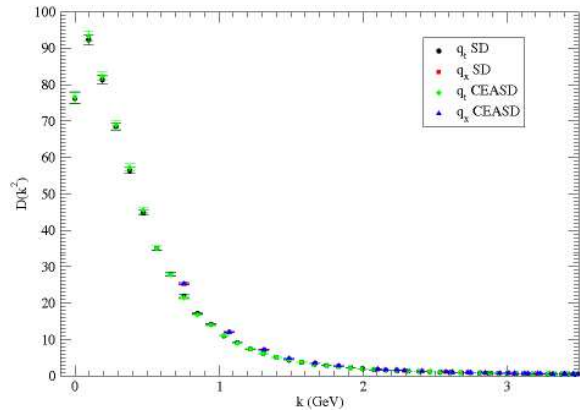Gribov copies are observed on the gluon propagator.

Fig. 2. Bare gluon propagator for $16^3 \times 128$.

3 Ghost propagator

The ghost propagator [13] was computed using two differ-
ent methods [14,15]. The first allows, by solving a linear
system, to access all momenta. Its drawback being that,
by computing $G(x, 0)$, the statistical errors in the prop-
agator are much larger. The second method requires an
inversion of the same linear system per momentum, which
is more computationally demanding. However, for the mo-
menta considered, it determines the propagator with bet-
ter statistical accuracy. Computing the propagator using
two methods provides a valuable cross-check.

In the following, for the ghost propagator the colour
average was always performed. For the propagator com-
puted with the [14] method, in order to reduce the sta-
tistical error, seven different sources for the linear system
were considered and their result averaged.

For the ghost propagator, one observes sizeable finite-
size effects (see fig. 3), in agreement with the $SU(2)$
study [16], and a very sign of clear Gribov copies effects
for a large range of momenta.

In what concerns finite volume effects, fig. 3 shows that
the ghost dressing function is enhanced when the lattice
volume is increased. Moreover, the larger volumes have a
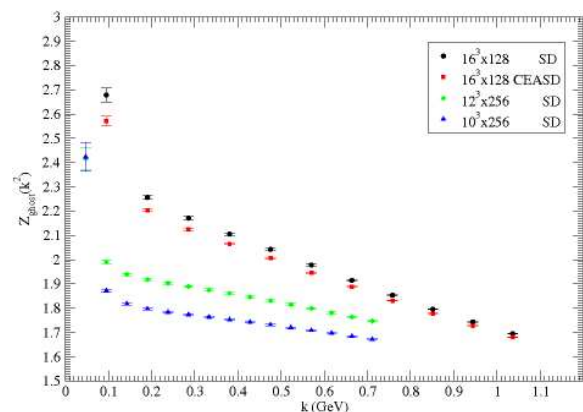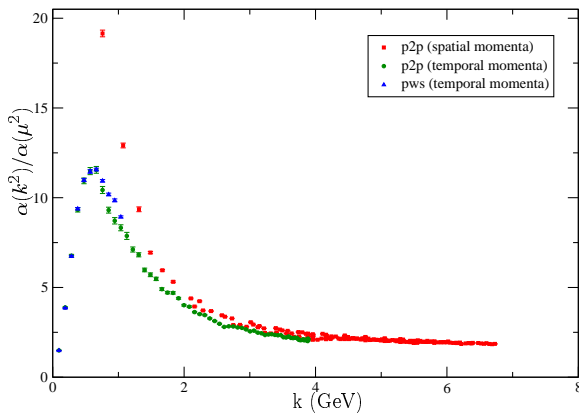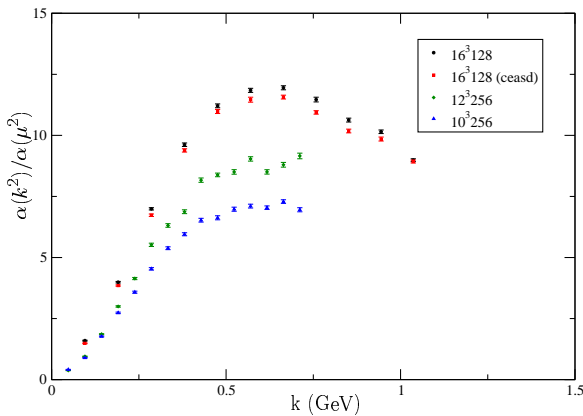larger dressing function and, for the smallest momenta,

Fig. 3. Bare ghost dressing functions for a $16^3 \times 128$ and
$L^3 \times 256$, $L = 10, 12$ lattices.

Fig. 4. Strong-coupling constant for $16^3 \times 128$ configurations for the CEASD gauge fixing method; "p2p" ("pws") stands for the ghost computed using [14] ([15]) method.

Fig. 5. Small-momenta strong coupling for all the simulations.

the derivatives of the dressing function seem to become smaller when the volume increases. The effect of Gribov copies, seen in fig. 3, cannot be eliminated by the renormalization of the propagator.

To study the compatibility of the ghost propagator with the DSE solutions, the lattice data was fitted to pure power laws and naïve corrections to the pure power law. It turns out that the data are not described by any of the functions considered. Given the results of a similar study for the $16^3 \times 128$ gluon propagator, this result is not a complete surprise.

4 Strong-coupling constant

The strong-coupling constant as defined by eq. (3) is displayed in fig. 4 for the $16^3 \times 128$ lattice and CEASD gauge fixing method. For the other simulations and the SD method, the measured coupling constants are, qualitatively, similar. Figure 5 shows the strong-coupling constant for small momenta, for all the simulations considered previously.

The simulations show a decreasing lattice strong-coupling constant for small momenta, in agreement with previous lattice calculations [17,18]. From our simulation, it is not clear if $\alpha_S(0)$ is vanishing. We have tried a number of fits to the strong-coupling constant as a function of the momentum, some requiring $\alpha_S(0) = 0$ and some leaving $\alpha_S(0)$ as a free parameter, and the data can be equally described by the two situations. For small momenta, only for the $16^3 \times 128$ data and the CEASD gauge fixing algorithm, is α_S described by a pure power law $\alpha_S(q^2) = (q^2)^{\kappa_\alpha}$, with $\kappa_\alpha = 0.69$ suggesting a vanishing strong-coupling constant at zero momentum. However, notice that the data show that α_S increases with lattice volume as seen in fig. 5 and is affected by Gribov copies. Further studies will hopefully lead to definitive conclusions.

References

1. For a review on strong-coupling constant see, for example, G.M. Prosperi, M. Raciti, C. Simolo, hep-ph/0607209.
2. L. von Smekal, A. Hauck, R. Alkofer, Phys. Rev. Lett. **79**, 3591 (1997); Ann. Phys. (N.Y.) **267**, 1 (1998).
3. C.S. Fischer, M.R. Pennington, Phys. Rev. D **73**, 034029 (2006).
4. For a review on DSE gluon and ghost propagators see, for example, C.S. Fischer, J. Phys. G **32**, R253 (2006) [hep-ph/0605173].
5. A.C. Aguillar, A.A. Natale, P.S. Rodrigues da Silva, Phys. Rev. Lett. **90**, 152001 (2003); A.C. Aguillar, A.A. Natale, JHEP **08**, 057 (2004).
6. Ph. Boucaud, J.P. Leroy, A. Le Yaouanc, A.Y. Lokhov, J. Micheli, O. Pène, J. Rodríguez-Quintero, C. Roiesnel, hep-ph/0507104.
7. C.S. Fischer, J.M. Pawlowski, hep-th/0609009.
8. O. Oliveira, P.J. Silva, AIP Conf. Proc. **756**, 290 (2005).
9. P.J. Silva, O. Oliveira, PoS (LAT2005) 286 (2006).
10. O. Oliveira, P.J. Silva, PoS (LAT2005) 287 (2006).
11. P.J. Silva, O. Oliveira, Phys. Rev. D **74**, 034513 (2006) [hep-lat/0511043].
12. O. Oliveira, P.J. Silva, Comput. Phys. Commun. **158**, 73 (2004) [hep-lat/0309184].
13. The definitions concerning the ghost propagator can be found in the articles where the lattice ghost propagator has been computed so far.
14. H. Suman, K. Schilling, Phys. Lett. B **373**, 314 (1996) [hep-lat/9512003].
15. A. Cucchieri, Nucl. Phys. B **508**, 353 (1997) [hep-lat/9705005].
16. A. Cucchieri, T. Mendes, Phys. Rev. D **73**, 071502 (2006) [hep-lat/0602012].
17. S. Furui, H. Nakajima, PoS (LAT2005) 291 [hep-lat/0509035]; hep-lat/0609024.
18. A. Sternbeck, E.-M. Ilgenfritz, M. Muller-Preussker, Phys. Rev. D **73**, 014502 (2006) [hep-lat/0510109]; **72**, 014507 (2005) [hep-lat/0506007].